



Behavior assessment of asymmetrical building with concrete damage plasticity (CDP) under seismic load

Patrick de Oliveira Batista da Costa

Federal University of Rio Grande do Sul - UFRGS, Brazil

patrick.costa@ufrgs.br, <https://orcid.org/0000-0002-2703-9875>

Rúbia Mara Bosse, Gustavo de Miranda Saleme Gidrão

Federal Technological University of Paraná - UTFPR, Brazil

rubiambosse@gmail.com, <https://orcid.org/0000-0003-4153-3455>

gustavo.gidrao@gmail.com, <https://orcid.org/0000-0003-1483-0526>

ABSTRACT. According to the research conducted, the asymmetric multi-storey buildings are complex and suffer from severe damage caused by increased torsional response. This paper addresses the behavior assessment of setback building with irregularity in the plan under severe seismic events such as Kobe earthquake. Using a three-dimensional model, the structure is subjected to seismic records in the three directions through ground accelerations. Nonlinear time-history analyses are employed to evaluate the dynamic response of the building. The mechanical model describes physical nonlinear behavior with evolution of damage and plasticity showing the regions of cracking propagation, mainly the columns-beams connections, corroborating the weak column and strong beam concept. The slabs did not present significant danification with damaged regions lumped on the borders of the first floors.

KEYWORDS. Dynamic nonlinear analysis; ABAQUS; Asymmetric building structure; Physical nonlinear behavior; Earthquake.



Citation: Costa, P. O. B., Bosse, R. M., Gidrão, G. M. S. Behavior assessment of asymmetrical building with concrete damage plasticity (CDP) under seismic load, *Frattura ed Integrità Strutturale*, 61 (2022) 108-118.

Received: 21.12.2021

Accepted: 21.04.2022

Online first: 26.04.2022

Published: 01.07.2022

Copyright: © 2022 This is an open access article under the terms of the CC-BY 4.0, which permits unrestricted use, distribution, and reproduction in any medium, provided the original author and source are credited.

INTRODUCTION

Real structures are almost always asymmetrical due the imperfections during execution process, architectonics design and innovation. Regarding buildings, the lack of symmetry tends to reduce the performance of structures subjected to seismic loads, thereby, leading to an increase in stresses of certain elements that consequently results in a significant destruction [1].

Buildings with elevation irregularities, e.g., setbacks, it is not uncommon to find considering that in large urban areas the space limitation is required, adequate ventilation and lighting to the lower floors and circulation areas. A lot of this buildings

are irregular in the plane as well, i.e., slab discontinuity and reentrant corners. Nevertheless, in contrast, major seismic codes distinguish between irregularity in the plan and in elevation [2].

The consideration of vertical seismic waves on the ground are required in irregular elevated buildings and with large spans due the significant change of the mass and e stiffness over the height of the building [3].

Torsion effect in asymmetric buildings in the plan are presented due the eccentricity of the mass and stiffness, therefore, the problem becomes more complex for multi-story structures [4].

This paper addresses the response of irregular setback building in the plane by means of seismic loading to the three directions. The dynamic analysis of spatial building under a three-component record of Kobe earthquake is developed through finite element method with ABAQUS CAE®.

In order to represent the behavior of the concrete in the structure, a refined constitutive model of damage coupled with plasticity (i.e. Concrete Damage Plasticity) already known and successfully used in studies of three-dimensional concrete slabs and beams under static loading in Cuong-Le *et al.* [5], high performance fiber-reinforced concrete (UHPFRC) structures under seismic loading in Sai Kubair and Kalyana Rama [6], and gravity dams under seismic loading in Zhang *et al.* [7], was used in this paper.

Solid 3D finite elements were used to represent the concrete material, steel reinforcements were totally embedded in concrete. Due the complexity of soil-structure interaction, the foundations and soils have not been modeled, hence, earthquake ground accelerations were applied to the base of columns in order to simulate a more realistic seismic event.

CONCRETE DAMAGE PLASTICITY

The physical nonlinear behaviour of concrete was represented by CDP already implemented in ABAQUS CAE® [8] involving the plasticity concepts with damage approached by Johnson [9], Wahalathantri *et al.* [10], Jankowiak and Lodygowski [11]. The model admits two failure mechanisms observed in Fig. 1 and 2.

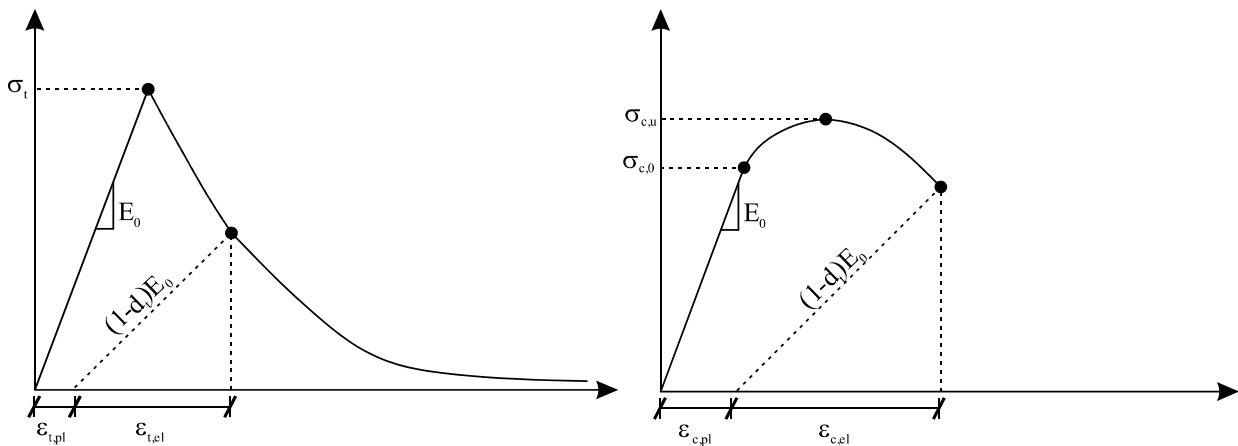


Figure 1: Uniaxial traction stress-strain response of concrete. Figure 2: Uniaxial compression stress-strain response of concrete.

This elastoplastic model allows the change from the uniaxial stress-strain curve to the plastic stress-strain curve accord with the equations below:

$$\sigma_t = (1 - d_t)E_0(\epsilon_t - \epsilon_t^{pl}) \tag{1}$$

$$\sigma_c = (1 - d_c)E_0(\epsilon_c - \epsilon_c^{pl}) \tag{2}$$

Correlating with Cauchy tensor of stress, it is possible to generalize to the multiaxial case:

$$\sigma = E_{el} : (\varepsilon - \varepsilon^{pl}) \tag{3}$$

$$E_{el} = (1 - d)E_0 \tag{4}$$

where $(\varepsilon - \varepsilon^{pl})$ are defined as the inelastic strain.

COMPRESSIVE BEHAVIOR

In this paper was used the analytical formulation for the stress-strain curve proposed by Carreira and Chu [12] which was used and successfully verified in some studies, such as the one presented by Ribeiro *et al.* [13]. This constitutive law was used as input in the CDP model, according to the following equations.

$$\frac{\sigma}{\sigma_0} = \frac{\beta \cdot \varepsilon / \varepsilon_0}{\beta - 1 + (\varepsilon / \varepsilon_0)^\beta} \tag{5}$$

$$\beta = \frac{1}{1 - \frac{\sigma_0}{\varepsilon_0 \cdot E_c}} \tag{6}$$

$$E_c = 25800 \cdot \left(\frac{f_{cm}}{10}\right)^{1/3} \tag{7}$$

$$\varepsilon_0 = 0.7 \cdot \frac{f_{cm}^{0.31}}{1000} \tag{8}$$

TENSILE BEHAVIOR

The tensile stress-strain curve was obtained according to formulation of Genikomsou and Polak [14], afterward Fig. 3. The value of G_f was computed according to the following equation, contained in item 5.5.5.2 of Model Code 2010 [15]. This Fig. 3 presents the tensile stress-strain law to concrete, used as input in concrete damaged plasticity model in ABAQUS CAE®.

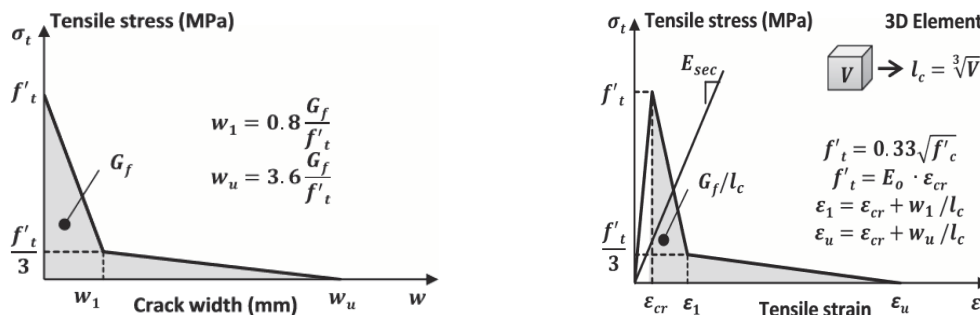


Figure 3: Analytical tensile stress-strain.

$$G_f = 73 \cdot (f_{cm})^{0.18} \tag{9}$$



NONLINEAR DYNAMIC ANALYSIS

According to Deierlein *et al.* [16] the nonlinear dynamic analysis in contrast to nonlinear static analysis provides more accurate response of the structure when subjected to a strong earthquake, furthermore the nonlinear dynamic analysis is most suitable due the building test model being complex, i.e., asymmetrical in plane and elevation. The enforced analysis was based on the temporal response, where the time-history of ground acceleration was selected from the Pacific Earthquake Engineering Research centre (PEER) database. Japan's famous 1995 earthquake was chosen regarding to its high moment of magnitude and peak ground accelerations purposing to get a better view of damage spread and structure behaviour. The recording characteristics of the accelerations in the three propagation directions are presented graphically in Fig. 4, and then the earthquake specifications are shown in Tab. 1.

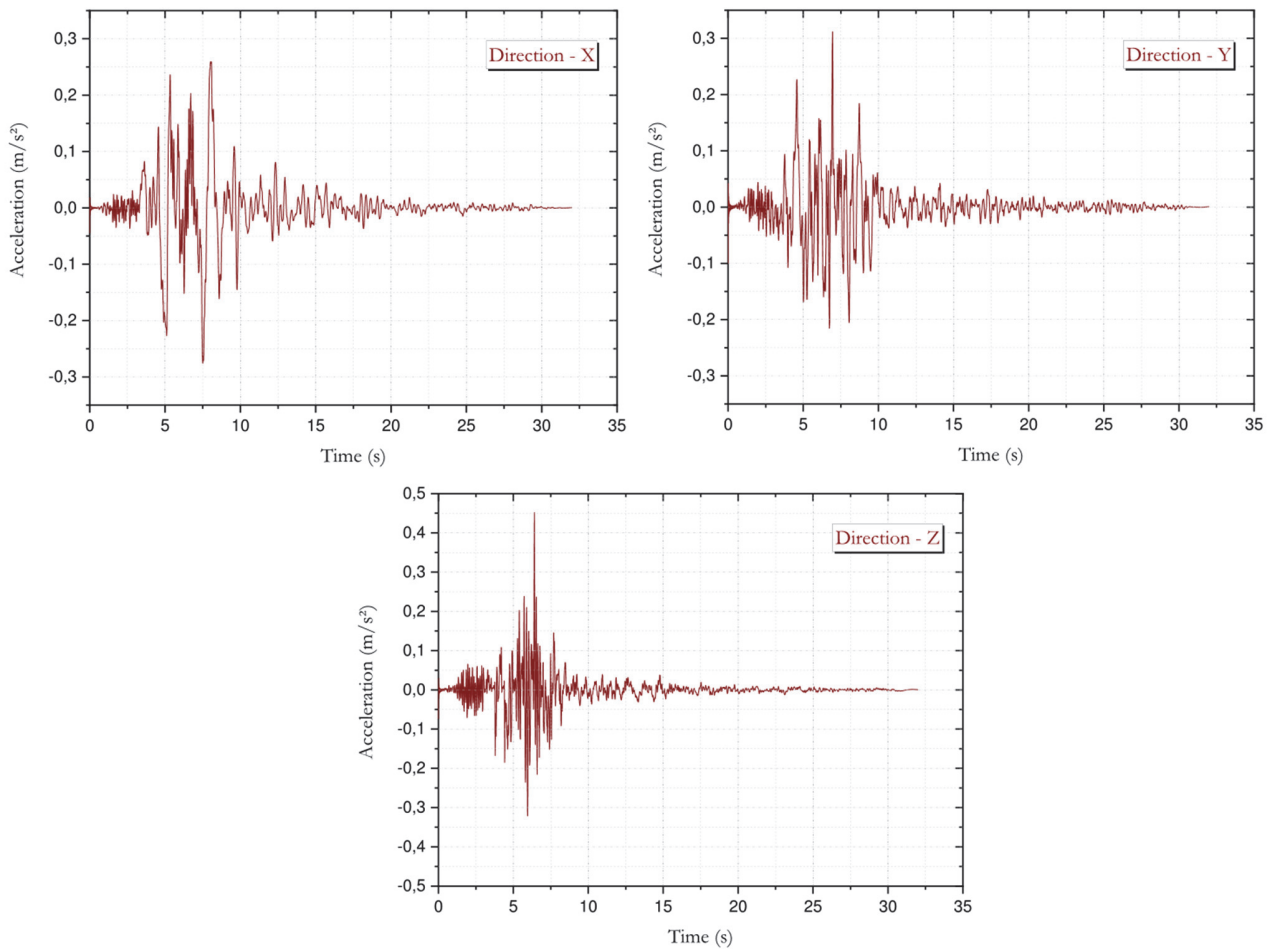


Figure 4: Accelerogram in the three earthquake directions.

Earthquake	Magnitude (Mw)	Hypocenter depth (km)	Direction	PGA (m/s^2)	T (s)
Kobe, Japan (1995)	6.9	17.9	X (plan)	-2.72	7.55
			Y (up)	4.52	6.40
			Z (plan)	3.12	6.95

Table 1: Characteristics of input motion data.

It is observed that the greatest acceleration on the ground is in the vertical direction, in addition the peak ground accelerations to the three directions are in close periods.

STUDIED CASE

The structure is a simplification of four-story building with irregularity in the plan and the elevation disregarding sealing masonry. The building is 14 meters high and represents a standard RC building designed in Brazil. In this study, it was subjected to a three-dimensional record of the Kobe earthquake. The density of concrete and steel are 2400 kg/m^3 and 7500 kg/m^3 , in order. Figs. 5 and 6 show the floor plan and cross sections details of the member. The slabs were modelled as a deformable diaphragm with concrete damage plasticity model as well, in addition, the slab's reinforcements were not considered just as the discontinuity of the diaphragm was also not considered in order to simplify the analysis.

The structure beam-column and slab were discretized with solid C3D8R elements, i.e., general purpose linear hexahedral element, fully integrated ($2 \times 2 \times 2$ integration points) present in the library provided by the software. The beam-column are reinforced with longitudinal and transversal by steel bars.

The reinforcements are modelled with B31 beam elements, i.e., three-dimensional element allowing transverse shear deformation with linear interpolation function present in the library provided by the software. The detail of the cross section of the beam as well as the reinforcement are illustrated in Fig. 7.

The concrete structures, longitudinal bars and stirrups have meshed with the same element size (100mm), This is due to the high computational cost of processing this type of analysis, although this mesh size did not cause high distortions in the elements, allowing for some acceptable accuracy.

The structural elements were modelled in separate parts (i.e., beams, slabs, columns and reinforcements), generating a 3D concrete frame. Then, the reinforcements were embedded into the concrete elements, through the "embedded region" interaction available in ABAQUS CAE®.

Dead loads are considered for all elements (with $g = -9,81 \text{ m/s}^2$). The building is subjected Kobe earthquake acceleration during 20 seconds. Loads were applied to the underside of the columns, thereby, seismic loading was propagated in the three directions, as shown the Fig. 8.

It is relevant to emphasize that the computation costs of this type of analysis can be demanding in the study. For the analysis of this structure it was necessary to reduce the earthquake time from 35 seconds to 20 seconds, and even then, it took 48 hours of processing, using three processors in parallel.

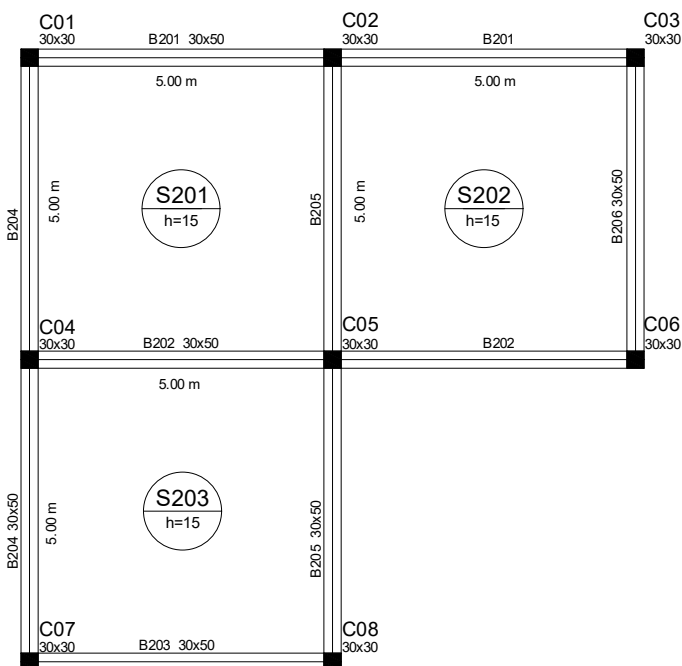


Figure 5: Plan of the test model.

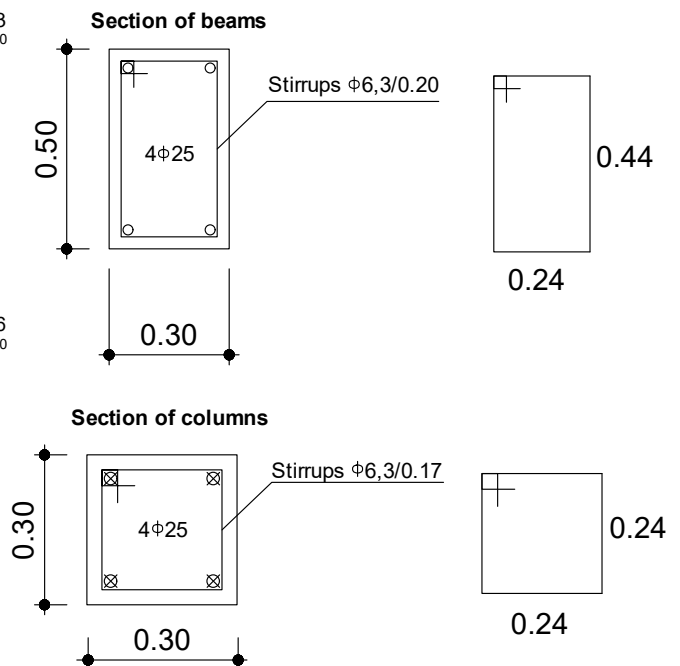


Figure 6: Member dimensions and reinforcement.

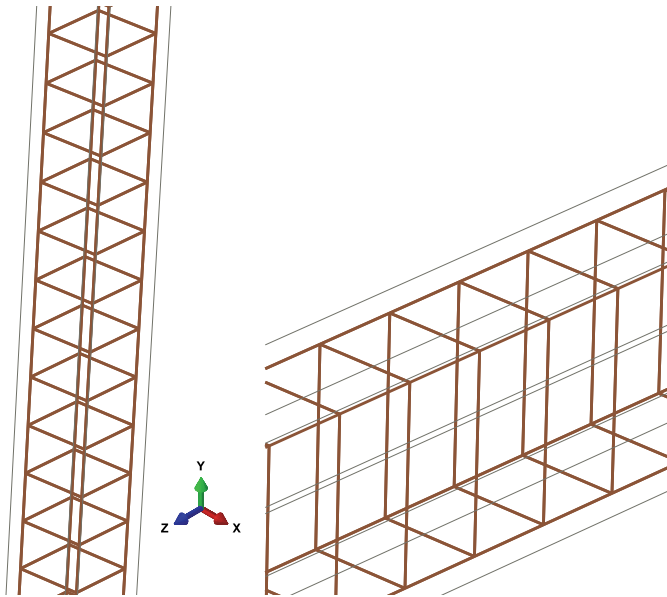


Figure 7: Steel reinforcements embedded in concrete.

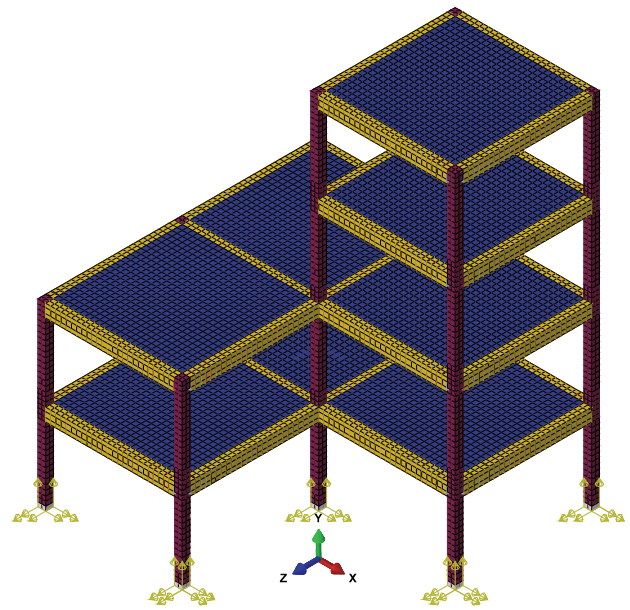


Figure 8: Displacements application point (meshed).

The properties of materials and parameters of the constitutive models in the elastic and plastic regime are observed in Tab. 2 and Tab. 3 respectively. The constitutive model of steel was considered perfectly plastic with yield stress equal 500 MPa. The average tensile strength of the concrete considered was 2.10 MPa.

Material	E_0 (GPa)	Compressive Strength (MPa)	Tensile Strength (MPa)
Concrete	21.5	30.0	0.20
Steel CA50	200.0	*	500.0

(*) the rupture of reinforcements was not considered in the model.

Table 2: Elastic properties of materials.

Material	Dilation angle (°)	Eccentricity	f_{b0}/f_{c0}	K	Viscosity
C30	45	0.10	1.05	0.667	0.0001

Table 3: Plastic properties of concrete.

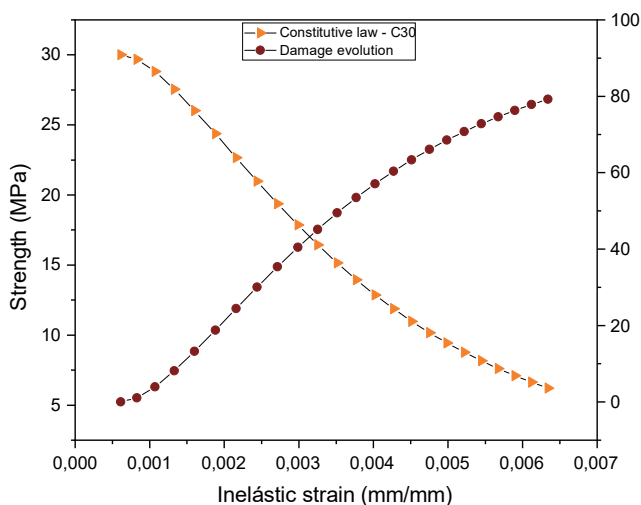


Figure 9: Constitutive law and damage evolution of C30 (compression).

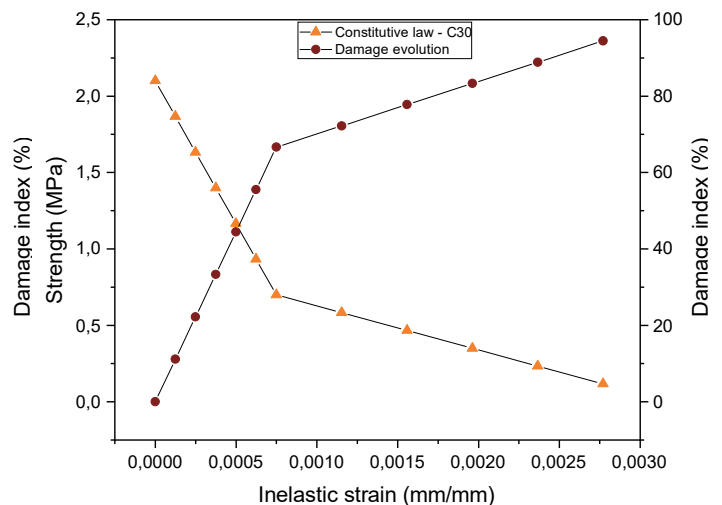


Figure 10: Constitutive law and damage evolution of C30 (traction).

The representation of the compressive and tensile constitutive relationship for this study are shown in Figs. 9 and 10 respectively, obtained by the analytical equations presented previously.

RESULTS AND DISCUSSIONS

Figure 11 presents the tensile damage in the concrete, where the beginning of the damage in 3.89 seconds may be observed. It is notable that the onset of tensile damage is presented only at the column bases and at columns whose zones are critical because the geometric center of the structure does not coincide with the center of rotation, e.g., reentrant corners.

In Figure 12 it can be seen that the damage is spreading along the structure, specifically the columns, already in the first few seconds of analysis. This occurs due to the accumulated earthquake energy being released.

It should be noted that for the same tensile strength of the concrete, tensile damage is prevalent in the columns than in the beams, because the stiffness of the columns is relatively lower compared to the beams due to their cross section.

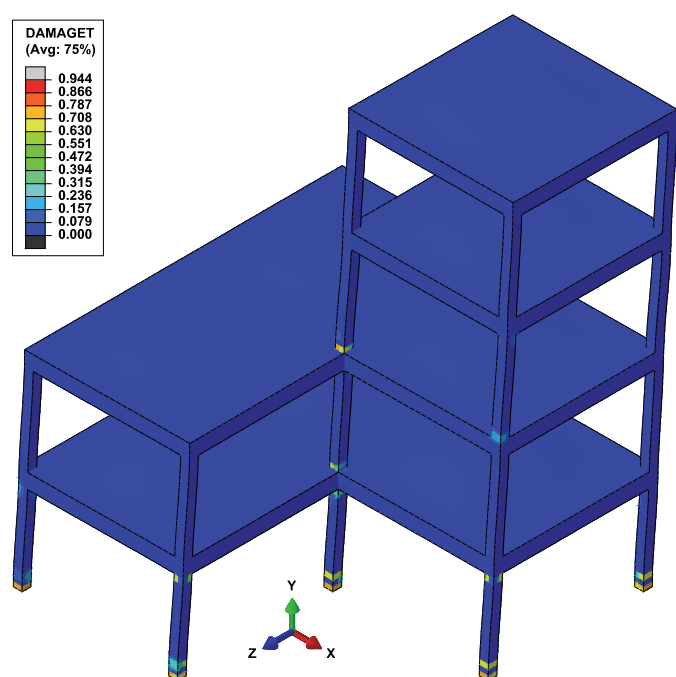


Figure 11: Damage at 3.89 seconds.

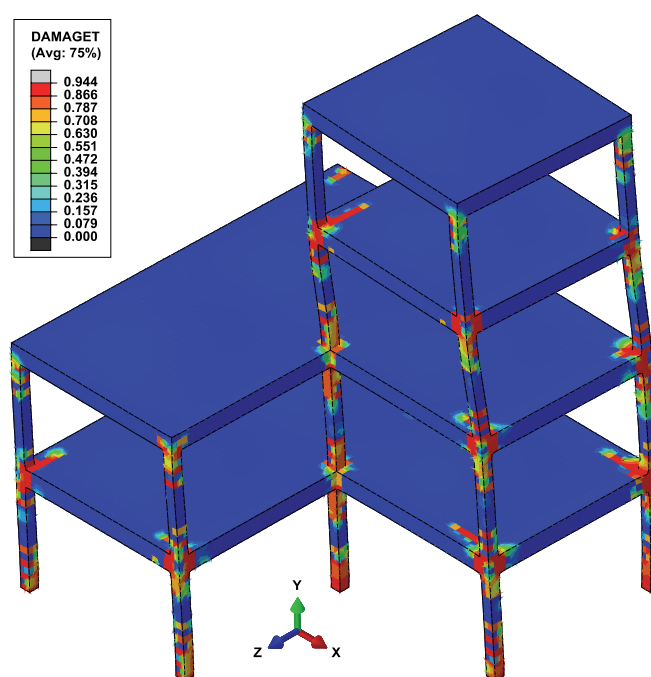


Figure 12: Tensile Damage at 5.51 seconds.

In Figure 13, the structure at 7.03 seconds of analysis was preferentially chosen because it is at this instant that starts a high energy release of the seismic due to the high peaks of accelerations in the three directions of propagation, thereby, it is evident the high concentration of damaged zones in the beam-column connections indicating the formation of plastic hinges, as expected. In addition, widespread damage occurs in the columns, thus proving the need for a strong and weak beam column configuration recommended by the literature and codes [17], otherwise there will be an instability problem of the structure, and it may be led to collapse.

It is possible to observe localized damage in the diaphragm and connected elements mainly in the second floor, and high stress concentrations in the corners of the floors, in which the collapse mechanism at the edges can be seen. However, the slab did not show damage and failure in the middle of the span. This proves that the slab worked well as a rigid diaphragm, due to its high stiffness in being massive, its thickness and its spans.

Figure 14 at 20.0 seconds represents the structure at the end of the analysis after all the energy during the seismic event has been released. Thus, it becomes clear that the RC building has come to ruin due to its deformation and especially the high damage in the region of the columns.

Another relevant aspect to note in Figure 14 is that the torsional effect becomes evident mainly in the corner columns, due to the asymmetry of the model's construction.

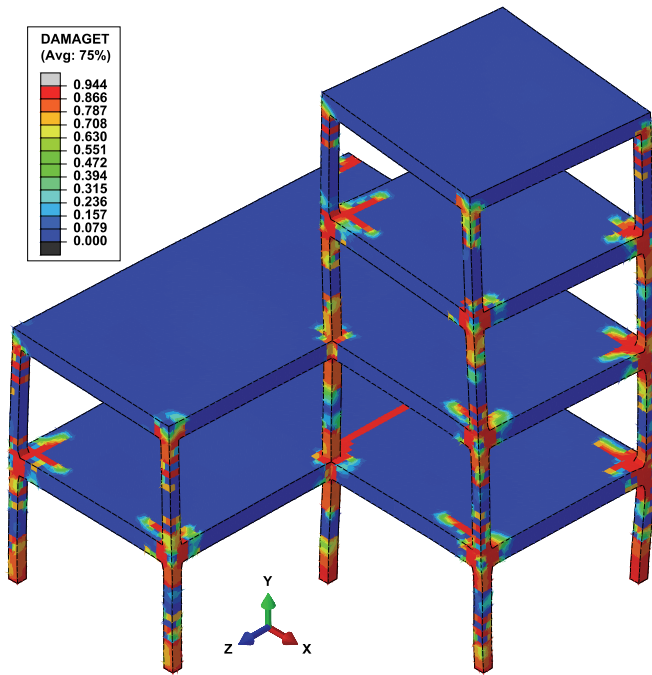


Figure 13: Tensile Damage at 7.03 seconds.

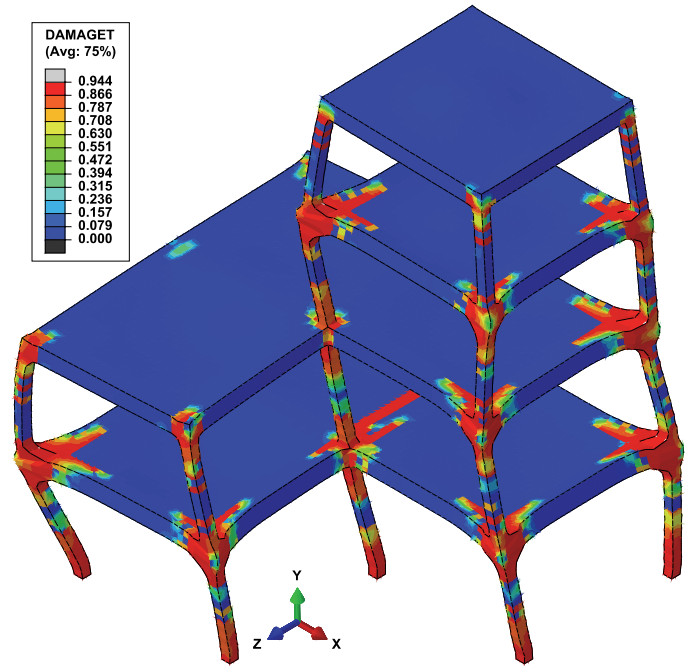


Figure 14: Tensile Damage at 20.00 seconds.

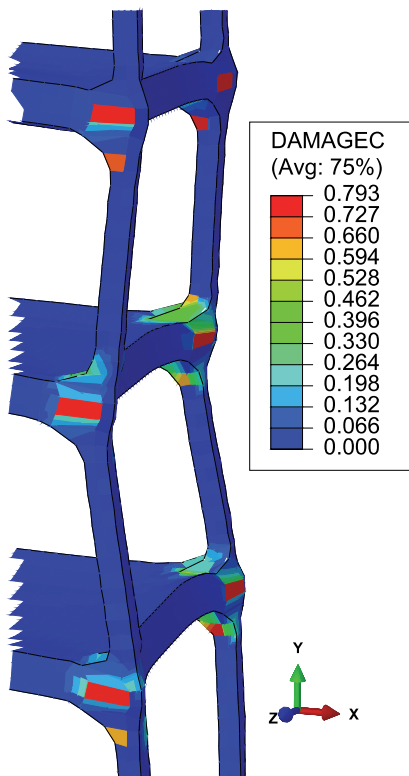


Figure 15: Compression Damage at 20.00 seconds.

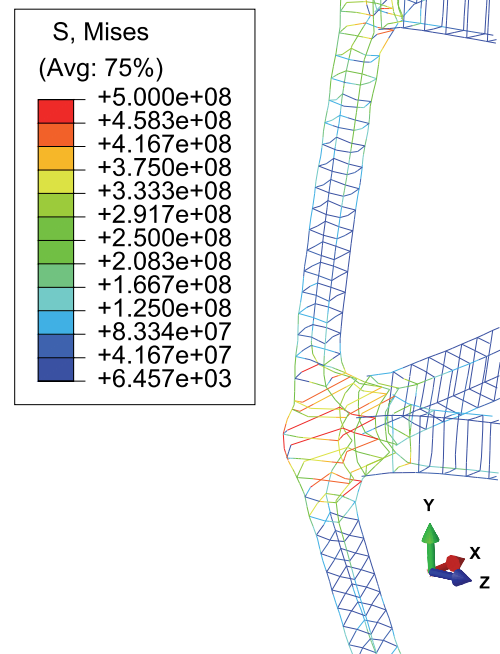


Figure 16: Strength in the reinforcements.

The Fig. 15 present the compression damage of the third-floor column-beam connection for the frame composed by C30 at 20.00 seconds, i.e., the end of the analysis. Even though concrete is a material that presents an excellent compressive

strength performance, in these regions of beam-column connection there is a need to increase concrete strength or increase the cross section of the columns, i.e., increase the effective area of concrete that contributes to compression.

Another relevant aspect evaluated in Fig. 15 refers to the quality of the mesh, as certain distortions in it are verified, requiring a more refined treatment for this region.

Afterwards, Fig. 16 shows the stress of steel reinforcements of the last-floor column-beam connection for the frame, where the maximum stress in structure reached values of 500 MPa, the yield stress for CA50 steel.

The plastic strain in corners reinforcements can be observed in the Fig. 17 due de beam-column connections.

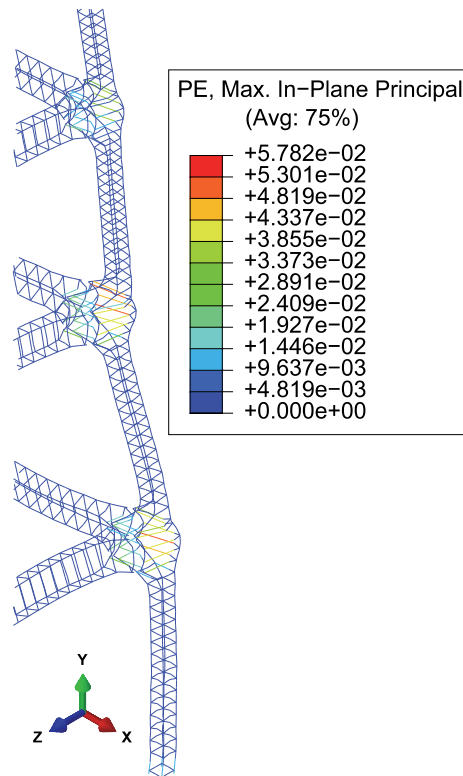


Figure 17: Plastic strain in the reinforcements.

CONCLUSIONS

The paper focused on the dynamic response of a realistic RC building, with irregular floor plan and elevation subjected to a single three component record of Kobe earthquake. Nonlinear time-history analyses were used with a mechanical model that considers the nonlinear behaviour of the materials estimating the evolution of damage due to cracking and plasticity in the concrete and in the reinforcement bars. Although the model presents high computational cost it is capable of representing complex realistic structures with flexural and torsional modes of vibration and the propagation of damage through the elements of beams, columns and slabs.

The main findings of the study were:

1. The results indicated that the building would present a collapse mechanism subjected to Kobe earthquake because all beam-column joints presented high levels of damage (on the order of 0.79 for tensile damage index) in the advanced stages of the earthquake. This phenomenon occurs due the progressive increase of bending moment along the connections, until the maximum bending moment is reached, where the connections lose their strength completely.
2. Before the maximum bending moment is reached, the damaged connections are capable to redistributing bending moments and shear forces along the neighbourhood, which is an advantage of the proposed simulation;
3. The slabs did not present evolution of damage along the span, indicating that the simplification of non-representing the reinforcement bars of the slabs in the FE models is suitable for the purpose of the analysis;



4. The structure did not present an acceptable performance to earthquake loads, showing a weak column and strong beam response. The model used to perform the analysis makes easy the observation of the failure modes and evidences the fragility of the structural elements. Several improvements in the design of the building can be punctuated, they are: to increase the concrete confinement zone, to adopt a higher reinforcements ratio for the stirrups in the critical zone, i.e., admitting a more ductile structure recommended by Eurocode [18] and American Concrete Institute [19] codes. It is important to emphasize that the Brazilian seismic code [20] does not address the detailing of seismic resistant structures.
5. In order to avoid the pathology generated due the re-entrant corners, the recommendation given by Federal Emergency Management Agency [21], i.e., to employ wide expansion joints between the connected slabs, increasing stiffness in the corners or launch of a rigid core over the structure seeking symmetry whenever possible.
6. The high computational cost of the proposed analysis prohibits its application to Performance Based Earthquake Engineering (ASCE/SEI [22]) approaches where a set of earthquakes with different intensities need to be imposed on the structure.
7. For future research, the authors suggest the mesh convergence test as well as its treatment for specific regions such as at the connections between elements and at stairwell and elevator openings, the inclusion of the influence of masonry interlock, and the contemplation of the effect of soil-structure interaction.

ACKNOWLEDGMENTS

The authors gratefully acknowledge the financial support provided CAPES (ID: 88887.607779/2021-00) and CNPq (ID: 131992/2021-0), Brazil.

REFERENCES

- [1] Mahdi, T. (2012). Static and Dynamic Analyses of Asymmetric Reinforced Concrete Frame. the 15th World Conference on Earthquake Engineering, Lisboa.
- [2] De Stefano, M., Pintucchi, B. (2007). A review of research on seismic behaviour of irregular building structures since 2002, *Bull. Earthq. Eng.* 6(2), pp. 285–308, DOI: 10.1007/S10518-007-9052-3.
- [3] Varadharajan, S., Sehgal, V.K., Saini, B. (2014). Seismic behavior of multistory RC building frames with vertical setback irregularity, *Struct. Des. Tall Spec. Build.*, 23(18), pp. 1345–1380, DOI: 10.1002/tal.1147.
- [4] Fernández-Dávila, V.I., Cruz, E.F. (2006). Parametric study of the non-linear seismic response of three-dimensional building models, *Eng. Struct.*, 28(5), pp. 756–770, DOI: 10.1016/J.ENGSTRUCT.2005.10.007.
- [5] Le Thanh, C., Minh, H.-L., Sang-To, T. (2021). A nonlinear concrete damaged plasticity model for simulation reinforced concrete structures using ABAQUS, *Frat. Ed Integrità Strutt.*, 16(59), pp. 232–42, DOI: 10.3221/igf-esis.59.17.
- [6] Sai Kubair, K., Kalyana Rama, J.S. (2022). Seismic Performance of UHPFRC-Strengthened RC Beam–Column Joints Using Damage Plasticity Model—A Numerical Study BT - Recent Advances in Earthquake Engineering. In: Kolathayar, S., Chian, S.C., (Eds.), Singapore, Springer Singapore, pp. 371–383.
- [7] Jiawen, Z., Mingchao, L., Shuai, H. (2022). Seismic Analysis of Gravity Dam–Layered Foundation System Subjected to Earthquakes with Arbitrary Incident Angles, *Int. J. Geomech.*, 22(2), pp. 4021279, DOI: 10.1061/(ASCE)GM.1943-5622.0002268.
- [8] Hibbitt, K. (2013). ABAQUS: User’s Manual: Version 6.13: Hibbitt.
- [9] Johnson, S. (2006). Comparison of Nonlinear Finite Element Modeling Tools for Structural Concrete, CEE561 Proj. Univ. Illinois Champaign, IL, USA.
- [10] Wahalathantri, B., Thambiratnam, D., Chan, T., Fawzia, S. (2011). A material model for flexural crack simulation in reinforced concrete elements using ABAQUS. Proceedings of the first international conference on engineering, designing and developing the built environment for sustainable wellbeing, Queensland University of Technology, pp. 260–264.
- [11] Jankowiak, T., Lodygowski, T. (2005). Identification of parameters of concrete damage plasticity constitutive model, *Found. Civ. Environ. Eng.*, 6(1), pp. 53–69.
- [12] Carreira, J and Chu, K.-H. (1985). Stress-Strain Relationship for Reinforced Concrete in Compression, *ACI Struct. J.*, pp. 797–804.



- [13] Ribeiro, P. de O., Gidrão, G. de M.S., Vareda, L.V., Carrazedo, R., Malite, M. (2020). Numerical and experimental study of concrete i-beam subjected to bending test with cyclic load, *Lat. Am. J. Solids Struct.*, 17(3), pp. 1–20, DOI: 10.1590/1679-78255880.
- [14] Genikomsou, A.S., Polak, M.A. (2015). Finite element analysis of punching shear of concrete slabs using damaged plasticity model in ABAQUS, *Eng. Struct.*, 98, pp. 38–48, DOI: 10.1016/j.engstruct.2015.04.016.
- [15] Concrete, If. (2013). *Fib Model Code for Concrete Structures 2010*, Ernst Sohn Publ. House .
- [16] Deierlein, G.G., Reinhorn, A.M., Willford, M.R. (2010). Nonlinear structural analysis for seismic design, *NEHRP Seism. Des. Tech. Br.*, 4, pp. 1–36.
- [17] Moehle, J.P., Hooper, J.D., Lubke, C.D. (2008). *Seismic design of reinforced concrete special moment frames: a guide for practicing engineers*. NEHRP Seismic Design Technical Brief, 1.
- [18] Bisch, P., Carvalho, E., Degee, H., Fajfar, P., Fardis, M., Franchin, P., Kreslin, M., Pecker, A., Pinto, P., Plumier, A. (2012). *Eurocode 8: seismic design of buildings worked examples*, Luxemb. Publ. Off. Eur. Union.
- [19] Committee, A.C.I. (2005). *Building code requirements for structural concrete (ACI 318-05) and commentary (ACI 318R-05)*, American Concrete Institute.
- [20] NBR, A. (2006). 15421: Projeto de estruturas resistentes a sismos-Procedimento, Rio Janeiro.
- [21] Council, B.S.S. (2003). *National Earthquake Hazards Reduction Program Recommended Provisions for Seismic Regulations for New Buildings and Other Structures (FEMA-450), Part 1: Provisions*, Fed. Emerg. Manag. Agency, Washington, DC, 303.
- [22] Engineers, A.S. of C. (2017). *Minimum design loads and associated criteria for buildings and other structures.*, American Society of Civil Engineers.

LIST OF SYMBOLS

d	damage index
d_t	damages in traction with values between [0,1]
d_c	damages in compression with values between [0,1]
ε	tensor of total strains
ε_0	strain related to σ_0
ε^{pl}	tensor of plastic strains
ε_t^{pl}	plastic strains in traction
ε_c^{pl}	plastic strains in compression
ε_t^{el}	elastic strains in traction
ε_c^{el}	elastic strains in compression
E_0	initial elasticity modulus
E_c	elasticity modulus
E_{el}	damaged elastic stiffness
f_{cm}	compressive strength
G_f	fracture energy
σ_0	maximum compressive stress
σ_{t0}	maxim traction stress and its respective elasticity limit
σ_{c0}	limit of elasticity for uniaxial compression
$\sigma_{\varepsilon,u}$	maxim compressive stress